

SUPERPOSITION OF DIFFUSION AND CHEMICAL REACTION CONTROLLED LIMITING CURRENTS - APPLICATION TO CO₂ CORROSION

by

Srdjan Nestic[‡], B.F.M. Pots[#], John Postlethwaite* and Nicolas Thevenot[‡]

Abstract

It was observed experimentally that a chemical reaction limiting current can be affected by flow. In the present study a new more general expression than the one found in literature was derived for the superposition of the diffusion and chemical reaction controlled limiting currents. It was found that their interaction in the case of CO₂ corrosion is significant at temperatures lower than 40°C and velocities higher than 1 m/s when the mass transfer layer is of the similar thickness as the reaction layer.

Introduction

The corrosion of steel in water containing dissolved CO₂ gas is a topic of considerable interest with practical applications and substantial economic impact in the oil and gas production and transportation industry.¹ When dissolved in water, the CO₂ is hydrated to give carbonic acid:



This weak, partly dissociated acid is responsible for high corrosion rates of steel in water CO₂ solutions. The electrochemistry of CO₂ corrosion is still not certain although a number of good studies exist in this field.²⁻⁸ One of the simplest assumptions is that the dominant cathodic reaction is the reduction of hydrogen ions, where the hydrogen ions are supplied by dissociation of carbonic acid:



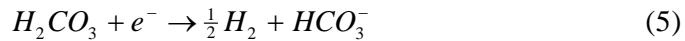
[‡] Institute for Energy Technology (IFE), P.O.Box 40, N-2007 Kjeller, Norway, e-mail: srdjan@ife.no

[#] Koninklijke/Shell-Laboratorium, Amsterdam (Shell Research B.V.), P.O.Box 38000, 1030 BN Amsterdam, The Netherlands, e-mail: pots1@ksla.nl

* IFE, on sabbatical leave from the University of Saskatchewan, Saskatoon, Canada, e-mail: John_Postlethwaite@enr.USask.Ca

[‡] Institute for Energy Technology (IFE), P.O.Box 40, N-2007 Kjeller, Norway, e-mail: srdjan@ife.no

The other possibility is the direct reduction of carbonic acid: ²



When conducting potentiodynamic sweeps on steel in CO₂ solutions, it is difficult to identify a pure Tafel region for the cathodic reaction as a limiting current is reached for relatively small overpotentials. The origin of this limiting current has been investigated ^{3,4} previously and is the topic of the present study.

Experimental

Equipment

Experiments were conducted at atmospheric pressure in a glass cell. Gas (CO₂ or N₂) was continuously bubbled through the cell. A three electrode set-up (Figure 1) was used in all electrochemical experiments. A rotating cylinder electrode with a speed control unit (0-5000 *rpm*)* was used as the working electrode. A concentric platinum ring was used as a counter electrode. A saturated Ag/AgCl reference electrode was used externally connected to the cell via a Luggin capillary and a porous wooden plug.. The speed of rotation of the working electrode was controlled with the aid of a stroboscope. The pH was followed with an electrode directly immersed into the electrolyte. The temperature was followed with a Pt-100 probe which also served as an input for the temperature regulating system - a hot plate combined with a magnetic stirrer. Oxygen concentration was monitored with an Orbisphere oxygen meter. The concentration of Fe⁺⁺ was measured occasionally using a photospectrometric method. The concentration of CO₂ in the water was also measured in selected experiments. Electrochemical measurements were made with a Gamry Instruments Inc. potentiostat connected with a PC 486/25 computer.

Material

A typical construction carbon steel St52 was tested (corresponding to ASTM A537 Grade 1). Chemical composition of the steel is given in Table 1. The working electrode was machined from the parent material into a cylinder 10 mm in diameter and 10 mm long. The exposed area of the specimen was 3.14 cm².

* 5000 *rpm* for our cylinder corresponds to a peripheral velocity of 2.61 *m/s* , a shear stress of 25 *Pa.*, and a Reynolds number of 26175.

Table 1. Chemical composition of the St52 steel used for the working electrode
(mass%)

C	Mn	Si	P	S	Cr	Cu	Ni	Mo	Al
0.130	1.25	0.35	0.022	0.004	0.12	0.31	0.08	0.02	0.035

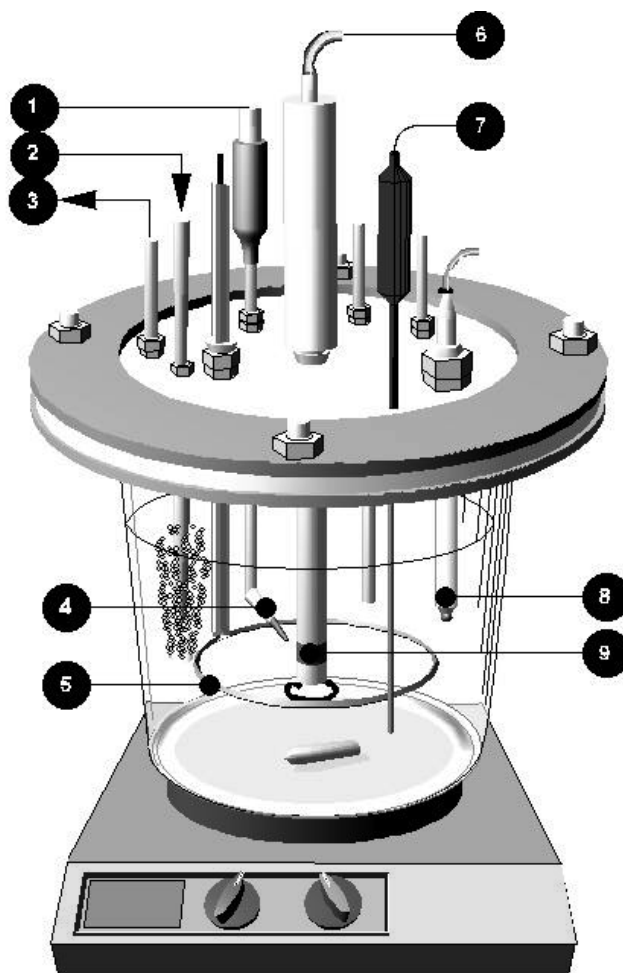


Figure 1. Schematic of the experimental test cell: 1-reference electrode, 2-gas in, 3-gas out, 4-Luggin capillary, 5-platinum counter electrode, 6-rotating cylinder, 7-temperature probe, 8-pH electrode, 9-working electrode.

Procedure

The glass cell was filled with 3 litres of electrolyte: distilled water + 1 mass% NaCl. In different experiments CO₂ or N₂ gas were bubbled through the electrolyte (min. 60 min.) in order to saturate or deaerate the solution. Monitoring of pH and O₂ concentration was used to judge when the solution was in equilibrium. When needed, HCl or NaHCO₃ were added to adjust the pH. The temperature was set and maintained with an accuracy of $\pm 1^\circ\text{C}$ in all experiments.

Before each polarisation experiment, the steel working electrode surface was polished with 500 and 1000 grit silicon carbide paper, washed with alcohol, mounted on the specimen holders and immersed into the electrolyte. The free corrosion potential was followed immediately after immersion. Depending on the conditions, the potential stabilised within ± 1 mV in 1 to 10 min.

The cathodic and anodic sweeps were conducted separately starting from the free corrosion potential. Typical scanning rate used was 0.1-0.2 mV/s. The cathodic sweeps were sometimes repeated by sweeping in the opposite direction, without significant difference in the result. In each experiment the anodic sweeps were conducted only once for a single working electrode specimen and a given electrolyte (starting from the free corrosion potential) since they altered the specimen surface and contaminated the electrolyte with significant amounts of dissolved iron ($\text{Fe}^{++} > 3$ ppm). Typically the Fe^{++} concentration was kept below 1 ppm.

Table 2. Experimental conditions

Test solution	water + 1 mass% NaCl
Test material	low carbon steel: St52
Temperature	22°C
Pressure	1 bar N_2 or CO_2
pH	4
Fe^{++}	<1 ppm
Dissolved oxygen	<20 ppb
Velocity	static - 10000 rpm
Test duration	0.5 hours
Sweep rate	0.1 - 0.2 mV/s
Potentiodynamic sweep	from -600 to +200 mV vs. E_{oc}
IR compensation	manual

Results

When conducting cathodic potentiodynamic sweeps in strong acids, limiting currents found are clearly flow dependent (Figure 2). It was shown previously⁹ that the rate of the hydrogen evolution reaction in the limiting current region proceeds only as fast as the hydrogen ions can diffuse from the bulk to the surface.

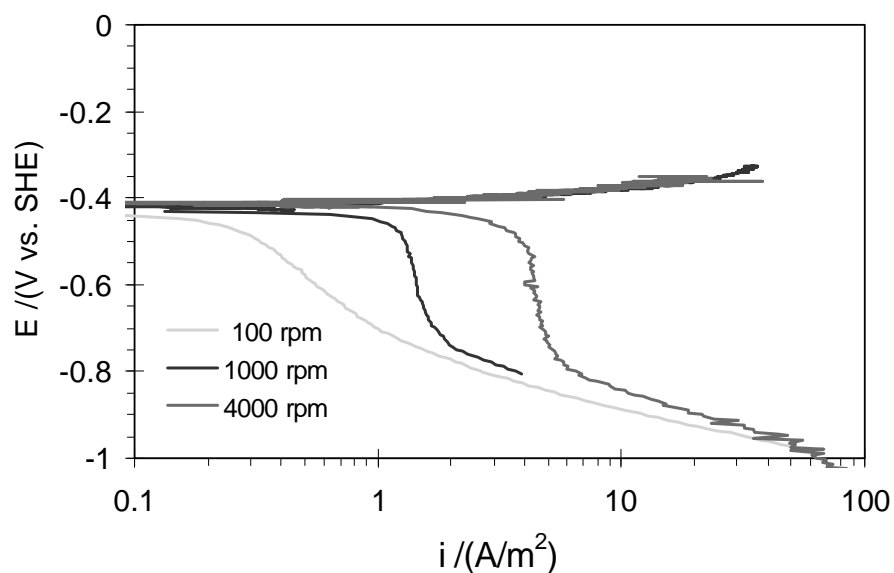


Figure 2. Potentiodynamic sweep conducted in HCl solution at pH 4 purged with N_2 , $t=22$ °C, 3% NaCl, using a rotating cylinder electrode $d=1$ cm.

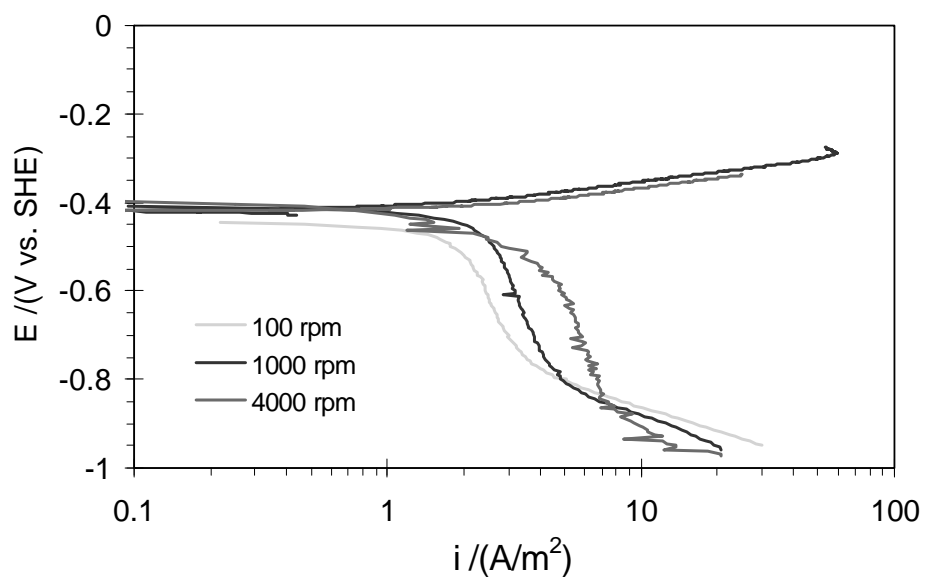


Figure 3. Potentiodynamic sweep conducted in a CO_2 solution at pH 4, $t=22$ °C, 3% NaCl, using a rotating cylinder electrode $d=1$ cm.

In CO_2 solutions it was found³ that the current limitation partly comes from a slow chemical step preceding the charge transfer step (see also Figure 3). It was assumed that the slow CO_2 hydration step (1) preceding the direct reduction of carbonic acid (5) is the cause for the observed limiting currents.

In the present study limiting currents were measured over the range of 500 - 10000 rpm in both HCl and CO_2 solutions using potentiodynamic sweeps. The correction was made for the contribution of the direct water reduction and the resulting limiting currents as a function of rotation speed are shown in Figure 4. The gap between the two curves which exists over the whole velocity range confirms the assumption of Schmitt and Rothman³ and Eriksrud and Sontvedt⁴ that there is a flow independent component of the limiting current in CO_2 solutions which is probably controlled by a chemical step: the hydration of CO_2 into H_2CO_3 .

If we assume that in CO_2 solution at pH 4, both the H^+ ions and H_2CO_3 are reduced at the surface, then at a given flow rate the limiting current for a CO_2 solution can be separated into two components. The first component is related to the diffusion of H^+ ions from the bulk (the same as in HCl solutions). The other flow independent (chemical reaction controlled) component which comes from H_2CO_3 is actually the gap between the two curves. Since the gap increases with rotation speed, it is hypothesised that the chemical reaction limiting current is also affected by the flow. This assumption will be analysed below.

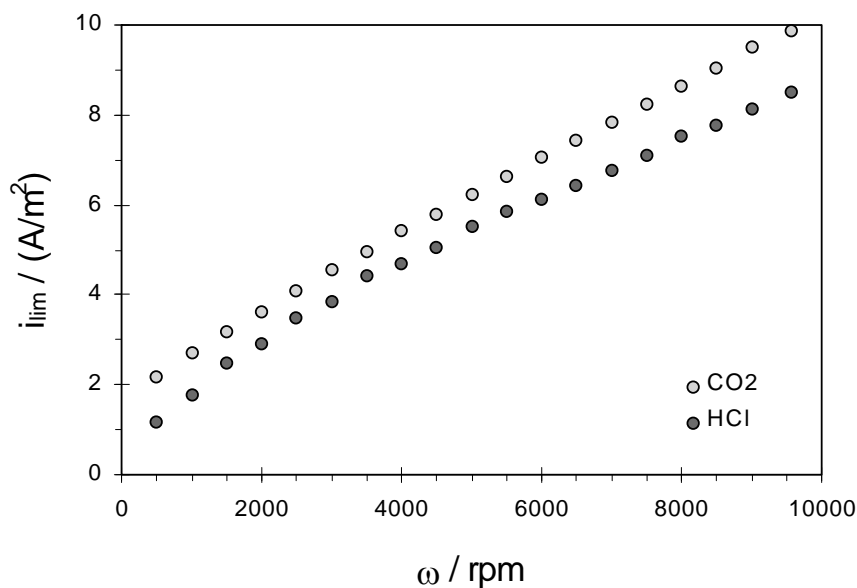


Figure 4. Limiting currents for a CO_2 and a HCl solution at pH4, $t=22^\circ\text{C}$ measured potentiostatically using a rotating cylinder electrode $d=1$ cm.

Discussion

Means for calculating the magnitude of a pure chemical reaction limiting current were first proposed by Vetter: ¹⁰

$$i_{\text{lim}(H_2CO_3)}^r = F\bar{c}_{H_2CO_3}\sqrt{k_{-1}D_{H_2CO_3}} \quad (6)$$

This equation was later successfully used to explain observed limiting currents in CO₂ solutions (glass-cell experiments). ^{5,11} However, it was recently reported ¹² that by using (6), limiting currents measured in loop experiments were underpredicted especially at higher velocities (>1 m/s). Inspection of Vetter's ¹⁰ derivation showed that (6) is strictly valid only for stagnant solutions when the thickness of the so-called "reaction layer" is much smaller than the thickness of the "diffusion layer". In that case the reported discrepancy ¹² can be explained by assuming that at higher velocities the thickness of diffusion layer was reduced and at some point became comparable to the thickness of the reaction layer. This concept is illustrated on Figure 5 where the calculated thickness of the two boundary layers are compared.

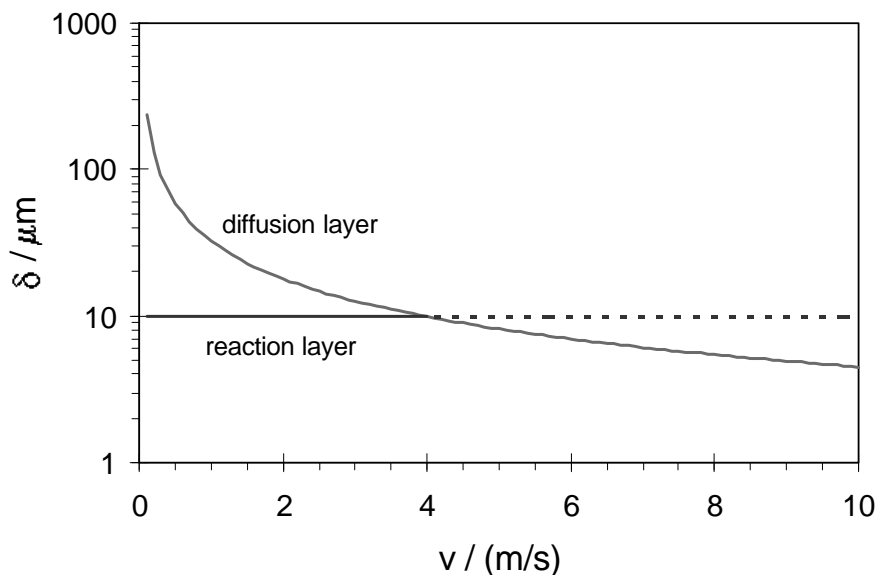


Figure 5. Thickness of the boundary layers for pipe flow, $t=20^\circ\text{C}$, $p\text{CO}_2=1 \text{ bar}$, $d_p=0.1\text{m}$.

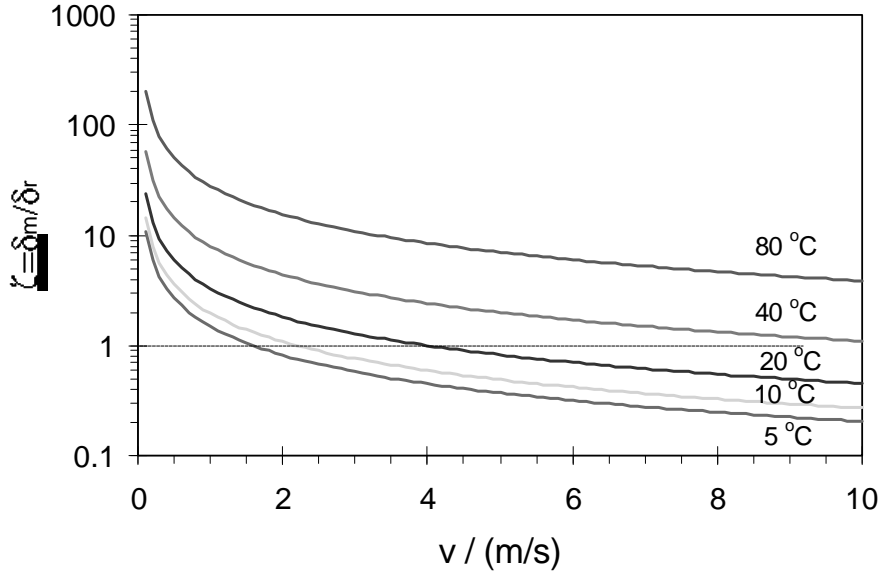


Figure 6. Boundary layer thickness ratio as a function of velocity and temperature for pipe flow, $p\text{CO}_2=1 \text{ bar}$, $d_p=0.1\text{m}$.

The thickness of the mass transfer (diffusion) layer δ_m shown in Figure 5 is estimated by using the relation:

$$\delta_m = \frac{D}{k_m} \quad (7)$$

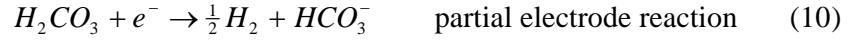
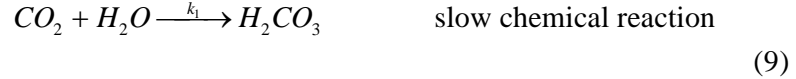
Here, D is the diffusion coefficient for carbonic acid and k_m is the mass transfer coefficient for straight pipe flow calculated using the correlation of Berger and Hau¹³. The thickness of the chemical reaction layer δ_r is calculated using the relation derived by Vetter¹⁰ for a first order chemical reaction:

$$\delta_r = \sqrt{\frac{D}{k_{-1}}} \quad (8)$$

where k_{-1} is the rate of carbonic acid dehydration (described in more detail below in the text). From Figure 5 it can be seen that under given conditions at 4 m/s the two boundary layers are of the same thickness. The ratio $\zeta = \delta_m/\delta_r$ is a strong function of temperature as shown in Figure 6. It is clear that for lower temperatures $\delta_m \approx \delta_r$ already for velocities larger than 1 m/s. Thus a more general expression than (6) is

needed for the reaction-controlled limiting current which accounts for any δ_m/δ_r ratio and covers a wider range of applications.

In order to derive such an expression, we will assume here the following sequence of reactions in the limiting current region:



If we further assume that reaction (9) is a first order chemical reaction, the rate of change of H_2CO_3 concentration is:

$$v = \underbrace{k_1 c_{CO_2}}_{\text{hydration}} - \underbrace{k_{-1} c_{H_2CO_3}}_{\text{dehydration}} \quad (11)$$

We can assume that the concentration of dissolved CO_2 is constant for all practical purposes and denote the rate of hydration with $v_o = \text{const.}$. For the sake of simplicity we can drop the subscript H_2CO_3 so (11) becomes:

$$v = v_o - k_{-1}c \quad (12)$$

At equilibrium $v=0$, hence:

$$v_o = k_{-1}\bar{c} \quad (13)$$

where \bar{c} is the equilibrium concentration of H_2CO_3 . Substitution of (13) into (12) gives:

$$v = v_o \left(1 - \frac{c}{\bar{c}}\right) = v_o(1 - u) \quad (14)$$

Here u is the nondimensional concentration of H_2CO_3 . It is the gradient of u (concentration) at the metal surface that will give us the desired chemical reaction limiting current.

To obtain the concentration profile the steady state mass balance (Fick's second law) for the case of an accompanying homogeneous chemical reaction has to be solved:

$$\frac{\partial c}{\partial t} = \frac{\partial}{\partial x} \left(D \frac{\partial c}{\partial x} \right) + v \quad (15)$$

For a steady state case $\partial c/\partial t = 0$. We can further assume that the diffusion coefficient is independent of concentration: $D \neq f(c)$ and that there are no temperature gradients so $D \neq f(x)$. Finally, by substituting v from (14) into (15), the nondimensional steady state mass balance is obtained:

$$\frac{\partial^2 u}{\partial x^2} + \frac{(1-u)}{\delta_r^2} = 0 \quad (16)$$

The boundary conditions are:

- at the metal surface, in the limiting current case, the concentration of H_2CO_3 is approaching zero, so for

$$x = 0 \quad \Rightarrow \quad u = \frac{c}{\bar{c}} = 0 \quad (17)$$

- for the bulk of the fluid due to turbulence the fluid is well mixed so there are no concentration gradients and we can assume that all reactions are in equilibrium, so for:

$$x = \delta_m \quad \Rightarrow \quad u = \frac{c}{\bar{c}} = 1 \quad (18)$$

Here we have assumed that the edge of the mass transfer boundary layer at $x = \delta_m$ is the point where everything is well mixed and all reactions are in equilibrium. At this stage the present derivation departs from the one in Vetter's¹⁰ book. Vetter¹⁰ assumes that the fluid is well mixed and in equilibrium only for $x \rightarrow \infty$ that is "very far" from the metal surface. This is a good assumption for stagnant solutions or laminar flow, however one can imagine that for a high enough velocity and turbulent flow the thickness of mass transfer layer δ_m is of the same order of magnitude as the reaction layer which we are calculating. Of course by setting $\delta_m \rightarrow \infty$ the present derivation follows the one in Vetter's¹⁰ book.

Integration of (16) with the boundary conditions (17) and (18) yields the nondimensional concentration profile:

$$u = 1 + \frac{e^{x/\delta_r}}{e^{2\delta_m/\delta_r} - 1} + \frac{e^{-x/\delta_r}}{e^{-2\delta_m/\delta_r} - 1} \quad (19)$$

We are interested in the limiting current which is:

$$i_{\lim(\text{H}_2\text{CO}_3)} = FD \left. \frac{\partial c}{\partial x} \right|_{x=0} = FD\bar{c} \left. \frac{\partial u}{\partial x} \right|_{x=0} = \frac{FD\bar{c}}{\delta_r} \cdot \frac{1 + e^{-2\delta_m/\delta_r}}{1 - e^{-2\delta_m/\delta_r}} \quad (20)$$

When $\delta_r = \sqrt{D/k_{-1}}$ is returned to (20) we obtain:

$$i_{\lim(\text{H}_2\text{CO}_3)} = F\bar{c} \sqrt{k_{-1}D} \cdot f \quad (21)$$

The original Vetter's¹⁰ expression (6) is now recovered, however corrected with the multiplier here called "flow factor":

$$f = \frac{1 + e^{-2\zeta}}{1 - e^{-2\zeta}} = \coth \zeta \quad (22)$$

which takes into account the effect of flow on the chemical reaction limiting current.

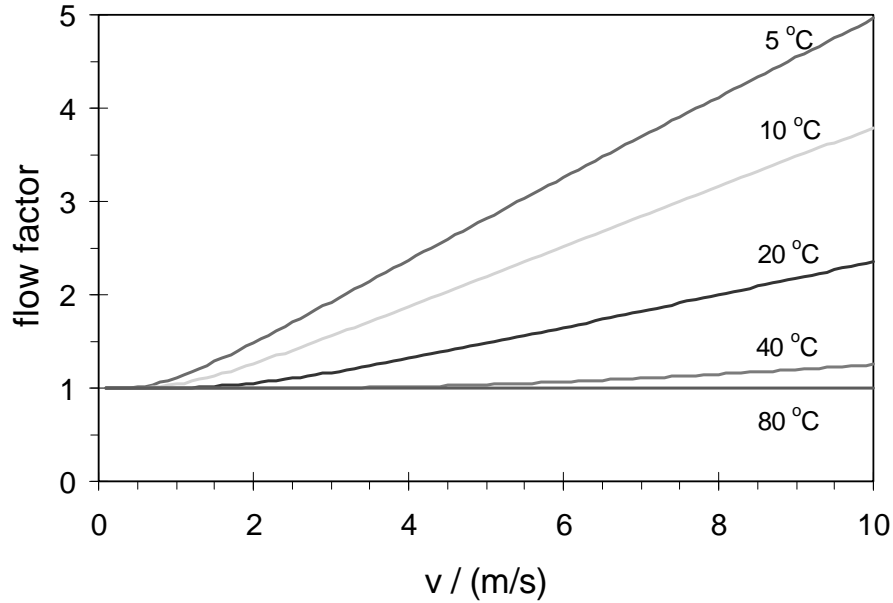


Figure 7. Flow factor as a function of velocity and temperature for pipe flow, $d_p=0.1$ m, $p\text{CO}_2=1$ bar.

Assuming a stagnant solution, $\zeta \rightarrow \infty$ so the flow factor $f=1$ and the solution reduces to the one derived by Vetter.¹⁰ The sensitivity of the flow factor to velocity and temperature is illustrated in Figure 7.

As a rule of thumb in CO_2 applications one can say that this correction is important for temperatures lower than 40°C and velocities higher than 1 m/s when the mass transfer layer is of the similar thickness as the reaction layer.

Another way of looking at the superposition of the diffusion and reaction limiting currents is to express it in terms of a pure diffusion limiting current corrected for the presence of a rate limiting chemical reaction¹⁴. By using (7) and (8) together with (21) it is obtained:

$$i_{\text{lim}} = k_m F \bar{c} \cdot \zeta \coth \zeta \quad (23)$$

Finally, the derived equations can be compared with the measured limiting currents shown in Figure 4. The result with and without the derived correction is shown in Figure 8. Although in the measured velocity range the effect is not large it is clear that the flow factor improves the agreement of the measurements and the theory.

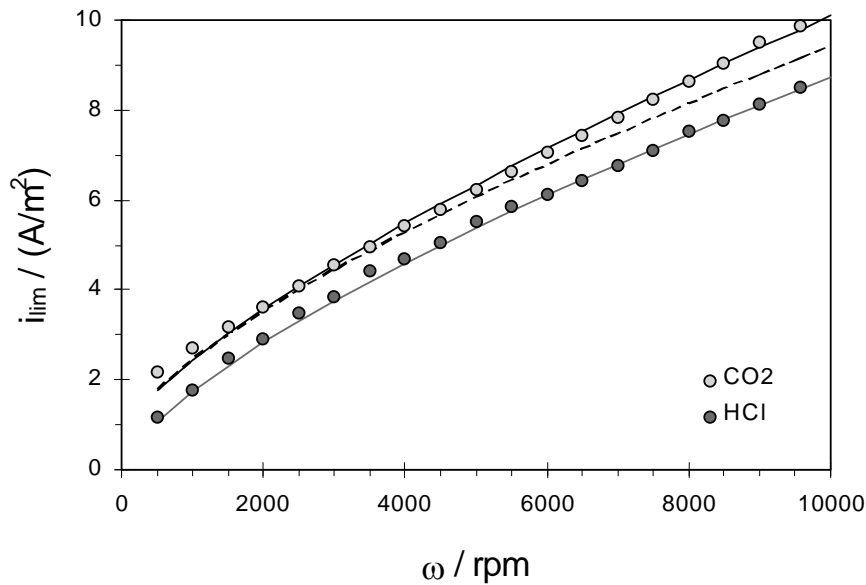


Figure 8. Comparison of the model prediction and experimental results. Conditions the same as in Figure 4. The points represent measurements, the lines are the model:

- mass transfer limiting current (Eisenberg et al. ¹⁵),
- mass transfer + chemical reaction limiting current (equation 6),
- mass transfer + corrected chemical reaction limiting current (equation 21).

Conclusions

It was observed experimentally that a chemical reaction limiting current can be affected by flow. A new more general expression was derived for the superposition of the diffusion and chemical reaction controlled limiting currents. It was found that their interaction in the case of CO_2 corrosion is significant at temperatures lower than 40°C and velocities higher than 1 m/s when the mass transfer layer is of the similar thickness as the reaction layer.

Nomenclature

c	concentration, mol/m^3 ;
\bar{c}	equilibrium concentration, mol/m^3 ;
D	diffusion coefficient, m^2/s ;
f	flow factor;
F	Faraday constant (96490 C/equiv.);

i_{lim}^r	chemical reaction limiting current density, A/m^2 ;
k_1	forward reaction rate (CO_2 hydration reaction), $1/s$;
k_{-1}	backward reaction rate (H_2CO_3 dehydration reaction), $1/s$;
k_m	mass transfer coefficient, m/s ;
u	nondimensional concentration;
v	chemical reaction rate, $\text{mol}/(s\ m^3)$;
x	distance from the metal surface, m ;
δ_m	thickness of the mass transfer (diffusion) layer, m ;
δ_r	thickness of the chemical reaction layer, m ;

$\zeta = \delta_m/\delta_r$ ratio of the diffusion and reaction layers;

References

1. A. Dugstad, L. Lunde and S. Nestic, "Control of Internal Corrosion in Multi-Phase Oil and Gas Pipelines", Proceedings of the conference Prevention of Pipeline Corrosion, Gulf Publishing Co., 1994.
2. C. deWaard and D. E. Milliams, Corrosion, 31 (1975): p.131.
3. G. Schmitt and B. Rothman, Werkstoffe und Korrosion, 28 (1977): p.816.
4. E. Eriksrud and T. Sontvedt, "Effect of Flow on CO_2 Corrosion Rates in Real and Synthetic Formation Waters", Advances in CO_2 Corrosion, Vol. 1. Proceedings of the Corrosion /83 Symposium on CO_2 Corrosion in the Oil and Gas Industry, Editors: R. H. Hausler, H. P. Goddard , p.20, (Houston, TX: NACE, 1984).
5. T. Hurlen, S. Gunvaldsen, R. Tunold, F. Blaker and P. G. Lunde, J. Electroanal. Chem., 180 (1984): p. 511.
6. L. G. S. Gray, B. G. Anderson, M. J. Danysh, P. G. Tremaine, "Mechanism of Carbon Steel Corrosion in Brines Containing Dissolved Carbon Dioxide at pH 4", Corrosion/89, paper no. 464, (Houston, TX: NACE International, 1989).
7. L. G. S. Gray, B. G. Anderson, M. J. Danysh and P. R. Tremaine, "Effect of pH and Temperature on the Mechanism of Carbon Steel Corrosion by Aqueous Carbon Dioxide", Corrosion/90, paper no. 40, (Houston, TX: NACE International, 1990).
8. M. R. Bonis and J. L. Crolet, "Basics of the Prediction of the Risks of CO_2 Corrosion in Oil and Gas Wells", Corrosion/89, paper no. 466, (Houston, TX: NACE International, 1989).
9. M. Stern, J.Electrochem. Soc., 102 (1955): p.609.

10. K. J. Vetter, *Electrochemical Kinetics, Theoretical Aspects*, Sections 1, 2, and 3 of *Electrochemical Kinetics: Theoretical and Experimental Aspects*, translation from German, (New York: Academic Press, 1967): pp.235-250.
11. S. Nescic, J. Postlethwaite and S. Olsen, “An Electrochemical Model for Prediction of CO₂ Corrosion”, *Corrosion/95*, paper no. 131, (Houston, TX: NACE International, 1995).
12. S. Nescic, G. Th. Solvi, and J. Enerhaug, “Comparison of the Rotating Cylinder and Pipe Flow Tests for Flow Sensitive CO₂ Corrosion”, *Corrosion/95*, paper no. 130, (Houston, TX: NACE International, 1995).
13. F. P. Berger and K.-F. F.-L Hau, *Int. J. Heat Mass Transfer*, 20 (1977): p.1185.
14. B. F. M. Pots, “Mechanistic Models for the Prediction of CO₂ Corrosion Rates under Multi-Phase Flow Conditions”, *Corrosion/95*, paper no. 137, (Houston, TX: NACE International, 1995).
15. M. Eisenberg, C. W. Tobias and C. R. Wilke, *J. Electrochem. Soc.*, 101 (1954): p. 306.